



Sensitivity of tidal lagoon and barrage hydrodynamic impacts and energy outputs to operational characteristics



Athanasios Angeloudis^{*}, Roger A. Falconer

Hydro-environmental Research Centre, School of Engineering, Cardiff University, The Parade, Cardiff, UK

ARTICLE INFO

Article history:

Received 6 May 2016

Received in revised form

9 August 2016

Accepted 11 August 2016

Available online 27 August 2016

Keywords:

Hydrodynamic modelling

Renewable energy

Tidal energy

Tidal lagoons

Tidal barrages

Resource assessment

ABSTRACT

The feasibility and sustainable operation of tidal lagoons and barrages has been under scrutiny over uncertainties with regards to their environmental impacts, potential interactions and energy output. A numerical modelling methodology that evaluates their effects on the hydro-environment has been refined to consider technical constraints and specifications associated with variable turbine designs and operational sequences. The method has been employed to assess a number of proposals and their combinations within the Bristol Channel and Severn Estuary in the UK. Operational challenges associated with tidal range power plants are highlighted, while also presenting the capabilities of modelling tools tailored to their assessment. Results indicate that as the project scale increases so does its relative hydrodynamic impact, which may compromise annual energy output expectations if not accounted for. However, the manner in which such projects are operated can also have a significant impact on changing the local hydro-environment, including the ecology and morphology. Therefore, it is imperative that tidal range power plants are designed in such a way that efficiently taps into renewable energy sources, with minimal interference to the regional hydro-environment through their operation.

© 2016 The Authors. Published by Elsevier Ltd. This is an open access article under the CC BY license (<http://creativecommons.org/licenses/by/4.0/>).

1. Introduction

Tidal range power plants are designed on the principle of creating an artificial tidal phase difference by impounding water, and then allowing it to flow through turbines to generate energy, in the form of electricity. The potential power (P) generated at any instant is proportional to the impounded wetted surface area (A) and the square of the water level difference (H) facilitated between the upstream and downstream sides of the impoundment:

$$P \propto A \cdot H^2 \quad (1)$$

Historically, the first large scale tidal range structure has been the La Rance barrage in France, in operation since 1966 [27]. This was followed by the 20 MW single turbine Annapolis Royal generating station in Canada (1984) and the more recent 254 MW Lake Sihwa tidal power station in South Korea [8]. Contrary to their successful performance for sustainable and predictable energy

production, there are mounting concerns over the environmental impacts induced by the presence of such renewable energy structures in estuarine and coastal waters. These impacts include alterations to the regional tidal flow characteristics, with interlinked effects on the local geomorphology, ecology and water quality processes [20,43].

The majority of the environmental impacts to-date have been accentuated through research and feasibility studies associated with a Severn Barrage, a prospective impoundment that has the potential of producing more than 5% of the UK's electricity needs [4,6,11,12,44–47]. It has been argued that due to the sensitive characteristics of the Bristol Channel and Severn Estuary, the introduction of such a structure would influence the established tidal resonance and flow structure in the basin; therefore, careful design becomes crucial. Earlier proposals failed to address the environmental and socio-economic concerns in a manner that maintained both the project feasibility and the operational efficiency beyond construction [31,32].

More environmentally friendly options are thought to be delivered through the tidal lagoon concept, where it is proposed that reduced disruption of the existing estuarine hydrodynamic

^{*} Corresponding author.

E-mail address: angeloudisa@cf.ac.uk (A. Angeloudis).

conditions will arise [6,14,41,42]. Tidal lagoons effectively operate on the same principles as tidal barrages. Their primary difference is that the majority of the impounded area perimeter is artificial, which enables their development in less environmentally sensitive locations compared to barrages, with the latter mainly restricted to estuary mouths and spanning the entire coastal basin width.

The assessment of tidal impoundments relies on the development of numerical tools that can simulate their operation over time. These span from simplified theoretical and zero-dimensional models [6,25,26,50]; to more sophisticated multi-dimensional hydro-environmental tools [6,12–14,36,44–48] that often require High Performance Computing (HPC) capabilities [43] to be practically applicable.

Results from a refined 2-D hydrodynamic modelling investigation, tailored specifically to tidal power plant assessment, are expounded upon in this study. The aims of this paper are therefore to: (a) review the methodology adopted for the operational simulation over transient conditions, (b) quantify and illustrate the cumulative hydrodynamic impacts of coastally-attached tidal lagoons and a barrage in estuarine flows, and (c) calculate the respective annual energy generation potential for various combinations with particular emphasis on proposals for the Severn Estuary and Bristol Channel.

2. Methodology

Starting from first principles and neglecting losses, the maximum potential energy over the course of a tidal period can be given by Ref. [25]:

$$E_{max} = 4\rho g A h_a^2 \quad (2)$$

where g is the gravitational acceleration ($= 9.807 \text{ m/s}^2$), ρ the water density ($\approx 1025 \text{ kg/m}^3$), h_a the tidal amplitude and A the impounded basin wetted area. According to Prandle's theory, an initial estimate of the actual extractable energy per tidal cycle corresponds to $0.27 \times E_{max}$ and $0.37 \times E_{max}$ for ebb-only and two-way generation respectively. In practise, a more elaborate methodology that provides an insight to the impoundment performance over transient tidal conditions is required, as outlined below.

2.1. Hydraulic structure representation

The performance of tidal impoundments is dictated by the regulation and specifications of their constituent hydraulic

structures, i.e. turbines and sluices. While turbines provide the power generation facilities of the power plant, sluice gates supplement the transfer of water volume at certain stages of the operation, generating greater head potentials on the subsequent half or full tidal phase. A straightforward approach used to calculate the flow driven through a hydraulic structure by a water head difference H is by the orifice equation:

$$Q = C_d A_f \sqrt{2gH} \quad (3)$$

where Q is the flow rate in m^3/s , A_f the flow area in m^2 , and C_d the discharge coefficient, given the value of unity herein as recommended by Ref. [10] with more recent experimental results by Ref. [29] indicating that C_d values for certain sluice gate designs can exceed a value of 1 with superior performance. Further details about the sensitivity of tidal impoundment simulations to C_d can be found in Ref. [11]. Equation (3) has been extensively applied to model the behaviour of sluice gates (e.g. Refs. [44,47,48]) and turbines alike [4,49].

However, the representation of low head bulb turbines can be refined to incorporate the characteristics specific to their design, as in Ref. [13]. The speed of the turbine S_p is given by:

$$S_p = \frac{2 \cdot 60 \cdot f_g}{G_p} \quad (4)$$

where f_g is the electricity grid frequency and G_p the number of generator poles. The unit speed (n_{11}) of a double regulated bulb unit can be expressed as [3] [13]:

$$n_{11} = \frac{S_p \cdot D}{\sqrt{H}} \quad (5)$$

where D is the turbine diameter in m. The specific discharge Q_{11} is normally calculated as:

$$Q_{11} = \frac{Q}{D^2 \cdot \sqrt{H}} \quad (6)$$

Alternatively, Q_{11} can be represented as a function of n_{11} through the following empirical expressions [3]:

$$Q_{11} = \begin{cases} 0.0166 \cdot n_{11} + 0.4861 & \text{if } n_{11} < 255 \\ 4.75 & \text{if } n_{11} \geq 255 \end{cases} \quad (7)$$

As a result, equation (5) is transformed and the turbine flow rate Q is calculated as:

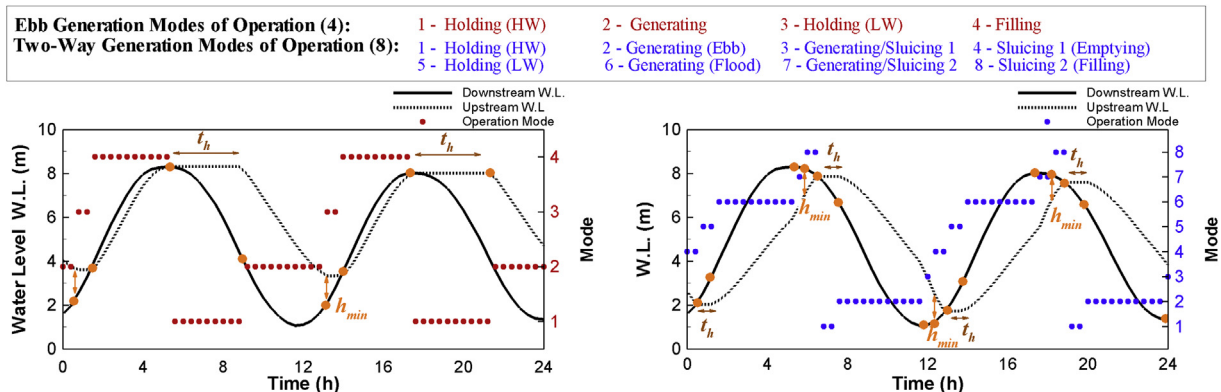


Fig. 1. Ebb-only and Two-way generation modes, illustrating upstream and downstream water levels over time as well as the trigger points that dictate the impoundment operation.

$$Q = Q_{11} \cdot D^2 \cdot \sqrt{H} \quad (8)$$

The turbine hydraulic efficiency η_h , according to the prototype of [3]; can be incorporated in the analysis as:

$$\eta_h = -0.0019 n_{11} + 1.2461 \quad (9)$$

In turn, other losses can also be accounted for, such as the: generator (η_p), transformer (η_t), gear box/drive train (η_g), water friction (η_w) efficiencies and turbine availability (η_a). Typical values adopted from previous studies are: $\eta_p = 97\%$, $\eta_t = 99.5\%$, $\eta_w = 95\%$, $\eta_g = 97.2\%$, $\eta_a = 95\%$ [50]. Thus, the power P produced at any instance for a given H is calculated as:

$$P = \rho g Q H \eta \quad (10)$$

where η is the overall efficiency factor. The number of generator poles (G_p), the turbine speed (S_p), and the grid frequency (f_g) can all be treated as constants. The remaining turbine parameters are variable and calculated as functions of H through equations 5–10, to produce representative hill charts based on available turbine specifications.

2.2. Operational sequences

Turbines and sluice gates are controlled over time according to the operational sequence selected for the tidal power plant. The operational sequence is governed by the approach proposed to generate power and can be during: ebb (ebb-only), flood (flood-only) or both ebb and flood (two-way) tides. However, it is practically limited by the impoundment design and hydraulic structure specifications. To-date, ebb-only or flood-only generation have been the standard sequences adopted for existing schemes (e.g. La Rance barrage and Lake Sihwa), mainly due to constraints at the sites of their development. Two-way generation is more attractive for ongoing proposal considerations, with a view to distributing the power generation function over a greater fraction of the tidal cycle. On the other hand, such an operation entails additional construction investment due to the need for expanded turbine caissons. In order to facilitate an efficient bulb turbine operation, a longer water passage is necessary for two-way generation than for one-way generation, as discussed by Ref. [9].

An ebb-only and a two-way sequence have been considered herein, as schematically demonstrated in Fig. 1 and using more information on the tidal plant operation from available relevant studies (e.g. Refs. [6,9,45]). The modes of operation, and how they are triggered over time, are summarised in Table 1, which describes the significant power plant functions over the course of a tidal cycle.

Additional considerations can be incorporated into the assessment methodology that reflect the plant operation. For example, in transitional periods, the discharge and power calculated are coupled with a ramp function $f_r(t)$. This represents the gradual opening and closing of the turbine wicket and sluice gates over a given duration (e.g. 20 min) as in Ref. [47]. Also, in two-way generation the power output from the turbines would be further influenced by their orientation; an efficiency factor ($\eta_o = 90\%$) has been imposed once turbines are generating in reverse, although this figure could be even lower in practise and particularly for complex inflow conditions.

For a potential site of known tidal hydrodynamics, the selected operational sequence in conjunction with the formulae adopted to represent the performance characteristics of the respective hydraulic structures is sufficient to simulate the overall performance of the lagoon or barrage. In the first instance, the operation can be

modelled using a water level time series as input, governed by the downstream water levels at the project location (Fig. 1). This is effectively the 0-D method and has been deemed sufficient under certain conditions [1,6,12,13,36]. However, this approach, though computationally efficient, assumes that the impact of the tidal impoundment itself on the localised tidal levels is negligible. This assumption can yield substantially overoptimistic results as the scale of the project increases [6,36]. Consequently, the analysis should be expanded to model the regional hydrodynamics to acknowledge the tidal impoundment influence on the hydro-environment and the adjacent water levels.

2.3. Hydrodynamic modelling

In the absence of stratification and three-dimensional patterns, the 2D shallow water equations can be employed for the prediction of estuarine tidal flow conditions as given by:

$$\frac{\partial U}{\partial t} + \frac{\partial E}{\partial x} + \frac{\partial G}{\partial y} = \frac{\partial \tilde{E}}{\partial x} + \frac{\partial \tilde{G}}{\partial y} + S \quad (11)$$

where U is the vector of conserved variables (i.e. mass, momentum and solutes), E and G are the advective flux vectors, while \tilde{E} and \tilde{G} are the diffusive vectors in the x and y directions respectively. S is a source term that can represent, among others, the effects of bed friction, bed slope and the Coriolis acceleration. The terms of Equation (11) can be expressed as:

$$U = \begin{bmatrix} h \\ hu \\ hv \end{bmatrix} \quad E = \begin{bmatrix} hu \\ hu^2 + \frac{1}{2}gh^2 \\ huv \end{bmatrix} \quad G = \begin{bmatrix} hv \\ huv \\ hv^2 + \frac{1}{2}gh^2 \end{bmatrix} \\ \tilde{E} = \begin{bmatrix} 0 \\ \tau_{xx} \\ \tau_{xy} \end{bmatrix} \quad \tilde{G} = \begin{bmatrix} 0 \\ \tau_{xy} \\ \tau_{yy} \end{bmatrix} \quad S = \begin{bmatrix} q_s \\ +hf v + gh(S_{bx} - S_{fx}) \\ -hf u + gh(S_{by} - S_{fy}) \end{bmatrix} \quad (12)$$

where u, v are the depth-averaged velocities (m/s) in the x and y directions respectively, h the total water depth (m) and q_s the source discharge per unit area. $f (= 2\omega \sin \varphi)$ refers to the Coriolis acceleration, where ω is the earth's angular velocity ($= 7.29 \times 10^{-5}$ rad/s) and φ the latitude within the domain. The variables $\tau_{xx} = 2h\nu_t(\partial u/\partial x)$, $\tau_{xy} = \tau_{yx} = h\nu_t(\partial u/\partial y + \partial v/\partial x)$, and $\tau_{yy} = 2h\nu_t(\partial v/\partial y)$, represent components of the turbulent shear stresses over the plane. The turbulent viscosity coefficient ν_t is given by $\nu_t = \beta u_* h$, where $\beta (=0.5)$ is a user-specified coefficient typically ranging from 0 to 1 and u_* is the friction velocity. The bed and friction slopes are denoted as $S_{bx} = -\partial Z_b/\partial x$, $S_{by} = -\partial Z_b/\partial y$ and $S_{fx} = n^2 u \sqrt{u^2 + v^2}/h^{4/3}$, $S_{fy} = n^2 v \sqrt{u^2 + v^2}/h^{4/3}$ for x and y directions respectively, where Z_b is the bed elevation in m and n the Manning roughness coefficient in $m^{-1/3}$ s. These expressions are imposed in the model as in Ref. [44] and included herein for completeness.

In the numerical model, computational domains are discretized into triangular cells to form unstructured meshes for the purposes of a cell-centred Finite Volume Method (FVM). Roe's approximate Riemann solver [28], including a Monotone Upstream Scheme for Conservation Laws (MUSCL) [39], resolves the normal fluxes across cell interfaces [18], following a predictor-corrector time stepping algorithm to satisfy second-order accuracy in time and space. The boundary conditions (i.e. land, water level and discharge

Table 1
Ebb-only and two-way modes of operation.

| Ebb-only modes of operation | | | | |
|-----------------------------|--------------------------------|--|---|--|
| m_1 | Mode | Hydraulic structure operation | Trigger conditions | Description |
| 1 | Holding (HW) | Turbines: Closed Sluice Gates: Closed | $Qt = 0$ $Qs = 0$ $m_0 = 4, H > 0$ $m_0 = 1, h_{st} > H > 0, t_m < t_h$ | Impounding water to facilitate a sufficient head (H) difference |
| 2 | Generating | Turbines: Generating Sluice Gates: Closed | $Qt < 0$ $Qs = 0$ $m_0 = 1, H > h_{st}, t_m < t_h$ $m_0 = 1, H > h_{min}, t_m > t_h$ $m_0 = 2, H > h_{min}$ | Generating Power at ebb tide by allowing flow through turbines, decreasing the upstream water level |
| 3 | Holding (LW) | Turbines: Closed Sluice Gates: Closed | $Qt = 0$ $Qs = 0$ $m_0 = 2, H < h_{min}$ $m_0 = 3, h_{min} > H > 0$ | Ceasing power generation due to lack of sufficient head difference (H) |
| 4 | Filling | Turbines: Open Sluice Gates: Open | $Qt > 0$ $Qs > 0$ $m_0 = 3, H < 0$ $m_0 = 4, H < 0$ | Operating turbines and sluice gates to maximize water level upstream for next cycle |
| Two-way modes of operation | | | | |
| m_1 | Mode | Hydraulic structure operation | Trigger conditions | Description |
| 1 | Holding (HW) | Turbines: Closed Sluice Gates: Closed | $Qt = 0$ $Qs = 0$ $m_0 = 8, H > 0$ $m_0 = 1, h_{st} > H > 0, t_m < t_h$ | Impounding water at High Water to facilitate a sufficient head (H) difference for ebb generation |
| 2 | Generating (Ebb) | Turbines: Generating Sluice Gates: Closed | $Qt < 0$ $Qs = 0$ $m_0 = 1, H > h_{st}, t_m < t_h$ $m_0 = 1, H > h_{min}, t_m > t_h$ $m_0 = 2, H > h_{min}, d\zeta_d/dt < 0$ | Generating Power at ebb tide by allowing flow through turbines, decreasing the upstream water level |
| 3 | Generating/Sluicing (Emptying) | Turbines: Generating Sluice Gates: Open | $Qt < 0$ $Qs < 0$ $m_0 = 2, H > h_{min}, d\zeta_d/dt > 0$ $m_0 = 3, H > h_{min}$ | Generating Power at ebb tide and allowing flow through sluice gates to further decrease upstream water level |
| 4 | Sluicing (Emptying) | Turbines: Open Sluice Gates: Open | $Qt < 0$ $Qs < 0$ $m_0 = 2, H < h_{min}$ $m_0 = 3, H < h_{min}$ $m_0 = 4, H > 0$ | Ceasing power generation due to lack of sufficient head difference (H) but continuing sluicing |
| 5 | Holding (LW) | Turbines: Closed Sluice Gates: Closed | $Qt = 0$ $Qs = 0$ $m_0 = 4, H < 0$ $m_0 = 5, -h_{min} < H < 0, t_m < t_h$ | Impounding water at Low Water to facilitate a sufficient head (H) difference for flood generation |
| 6 | Generating (Flood) | Turbines: Generating Sluice Gates: Closed | $Qt > 0$ $Qs = 0$ $m_0 = 5, H < -h_{st}, t_m < t_h$ $m_0 = 5, H < -h_{min}, t_m > t_h$ $m_0 = 6, H < -h_{min}, d\zeta_u/dt > 0$ | Generating Power at flood tide by allowing flow through turbines, increasing the upstream water level |
| 7 | Generating/Sluicing (Filling) | Turbines: Generating Sluice Gates: Open | $Qt > 0$ $Qs > 0$ $m_0 = 6, H < -h_{min}, d\zeta_u/dt < 0$ $m_0 = 7, H < -h_{min}$ | Generating Power at flood tide and allowing flow through sluice gates to further increase upstream water level |
| 8 | Sluicing (Filling) | Turbines: Open Sluice Gates: Open | $Qt > 0$ $Qs > 0$ $m_0 = 6, H > -h_{min}$ $m_0 = 7, H > -h_{min}$ $m_0 = 8, H < 0$ | Operating turbines and sluice gates to maximize water level upstream for next cycle |

m_1 = Mode of operation, m_0 = Mode of operation at previous time step, h_{st} = Desired head difference for turbine operation (m), h_{min} = Minimum head difference for turbine operation (m), t_m = Duration of current mode (h), t_h = maximum holding duration (h), ζ_d = Downstream water level, ζ_u = Upstream water level.

boundaries) are treated as in Refs. [30] and [33] with an integrated algorithm for wetting and drying processes in intertidal regions [16].

In terms of stability, the numerical model is based on a Total Variation Diminishing (TVD) scheme, which is an explicit algorithm and is therefore intrinsically stable, as long as the Courant-Friedrichs-Lewy (CFL) number is less than unity. Predicted hydrodynamics are therefore not susceptible to the generation of non-physical oscillations and are suitable for modelling the high velocity flows triggered through the turbine and sluice gate areas.

A domain decomposition approach is implemented to represent tidal power plants in the hydrodynamic model. This considers an upstream subdomain for each impoundment, connected to the downstream domain through open boundaries that are specified in the region of flow control structures. Subdomains are dynamically linked using a relationship between the discharge Q and the water head difference H at the boundary nodes through equations (3)–(8) and operated over time according to the sequences of Fig. 1 and Table 1. The representation of the hydrodynamic processes through

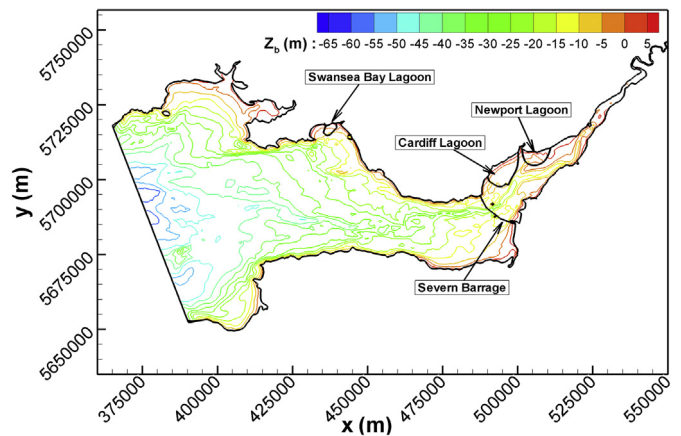


Fig. 2. Severn Estuary and Bristol Channel bathymetry and indication of tidal impoundment proposals and study domain boundaries (UTM coordinates).

the hydraulic structures is based on the supercritical flow boundary formulation as given in Refs. [5] and [7], to preserve the flow area and momentum through the turbines and sluices.

3. Tidal range power plant options in the Severn Estuary and Bristol Channel

There is substantial interest in harnessing power from the significant tidal range developed in the Bristol Channel and the Severn Estuary, in the UK. The methodology was employed to assess a number of potential tidal impoundments, with their location and outline being indicated in Fig. 2. These include previous and optimised versions of a Cardiff-Weston barrage and three tidal lagoon proposals, i.e. the Swansea Bay, Cardiff and Newport lagoons.

3.1. Project background

A barrage in the Severn Estuary has been the most discussed tidal range project in the UK, with the conceptual idea going back over a century [40]. Numerous variants have been proposed that have fallen short in terms of adequately addressing issues of concern, such as: the high construction cost and the satisfactory identification and mitigation of potential environmental impacts. One of the most detailed proposals considered was the STPG (1989) scheme; a Cardiff-Weston barrage (Fig. 2), consisting of 216×40 MW, 9.0 m diameter bulb turbines, 166 sluice gates and ship locks among other hydraulic structures. In order to contain construction costs, the STPG turbine caissons were solely designed for an ebb-only operation (Fig. 1).

The Swansea Bay Lagoon (Fig. 2) project was initiated by Tidal Lagoon Power Plc (2014) and proposed, at the time of writing, the construction of an artificial lagoon along the Swansea Bay coast to impound 11.6 km² for the purpose of tidal power generation. It builds upon an earlier 5 km² proposal by Tidal Electric Inc. in 2004, which however did not progress beyond the preliminary design stages [10]. The Swansea Bay Lagoon project has been granted planning consent and, if constructed, would have a potential installed capacity of 320 MW, provided by 16×20 MW, 7.35 m diameter bulb turbines. It would become the largest tidal range project to-date and, contrary to earlier proposals, it is designed to function through a two-way sequence to reduce power generation intermittency.

The proposed Swansea Bay lagoon is generally perceived as a pilot scheme for larger projects within the Severn Estuary and beyond (such as along the North Wales coast). These include the Cardiff and Newport Lagoons with current designs highlighted in Fig. 2. Their location has similarly been used for previous proposals, namely the Peterstone flats and the Welsh Grounds lagoons [51]. Both of the latter were dismissed during an earlier Department of Energy and Climate Change (DECC) review (2008). Nonetheless, they demonstrate the significant interest for deploying sustainable tidal energy projects in the region.

3.2. Tidal power plant numerical models

An appreciation of the regional tidal hydrodynamics and potential tidal range energy resource can be acquired through a coastal modelling methodology. Taking into account the large tidal range in the Bristol Channel and the Severn Estuary, it has been reported that the estuarine conditions are well-mixed and there is no evidence of stratification in the areas of interest [38], suggesting that the natural tidal dynamics are predominantly two-dimensional. Three-dimensional flow conditions will develop in the immediate locations downstream and upstream of the turbines and sluice gates, but for the regional scale modelling reported in the

paper these will be largely confined to the cells adjacent to the hydraulic structures, as shown by experimental investigations [19]. Therefore a high resolution 2-D modelling approach was considered suitable for the objectives of this study.

The Bristol Channel and Severn Estuary tidal conditions were previously modelled and validated, with details found in Xia et al.(2010c). It should be noted that for this particular basin the tide is known to amplify within the channel and estuary and attention needs to be given to changes in the tidal resonance characteristics as a result of any major project being considered in the basin. Hence changes to boundary conditions as a result of any large impoundments also need to be acknowledged by modelling the far field hydrodynamics right out to the continental shelf, and where the governing tide is generated. The seaward boundary of the computational domain for this study (Fig. 1) was set up as a water level boundary according to the tidal flow conditions in the region, which were provided by the National Oceanographic Centre, to cover both spring and neap tide conditions. The tidal harmonics are consistent and in line with the Continental Shelf Models of [49] and [11]; previously used to assess the effects of a Severn Barrage. For the Severn Barrage configurations herein, the seaward boundary conditions were defined according to the models of [11] that extend to the edge of the Continental Shelf, with their model set-up to focus on the far-field impacts of the particular project. Such a boundary treatment was essential to predict the effects of large-scale projects on the domain open boundary, as suggested by Refs. [17] and [2]. For the tidal lagoons which do not cross the estuary and directly impact on the tidal resonance characteristics, it was deemed that the simulation results were independent from the far-field open boundary conditions, but this assumption needs further analysis in the future. For the refined hydraulic structure treatment that replicates the relatively high velocities close to turbine regions [7], a higher resolution was imposed with an element size of 25 m close to areas of interest (Fig. 5), extending to 1000 m at the seaward boundary. The bathymetry of these models was interpolated using digitized data provided by Seazone Solutions with a resolution of 1 arc second. For stability, the maximum CFL number was consistently <1.0 for the simulations, using a time step of $\Delta t = 0.5$ s in all cases.

The reliability of the predictions is reaffirmed by comparisons between the refined Severn Estuary simulations against observed data throughout the period of 06/03/2005–06/04/2005. These include water level time series variations from the UK Tide Gauge Network, as shown in Fig. 3a–d, which covers the first 180h of the lunar month. Correlation coefficients R^2 of 0.992, 0.993, 0.994 and 0.994 and Root Mean Square Deviation (RMSD) values of 0.36, 0.34, 0.28 and 0.26 m respectively suggest a high level of agreement between both sets of results, which allows progression to the tidal impoundment assessment for a value of $n = 0.022$. It should be noted that the RMSD deviations are mostly attributed to discrepancies in the form of slight overestimations at the prediction of neap tides (Fig. 3) with better agreement being obtained during spring tidal conditions. A similar pattern was observed in earlier applications of the model [44] and can be attributed to some assumptions in the modelling methodology, such as the uniform Manning's number value imposed for simplicity.

The mean amplitude calculated from the month-long simulation at the proposed sites could, in turn, be used to calculate a preliminary estimate of the theoretical potential energy according to equation (2) as summarised in Table 2. The results in the table are meant to provide an appreciation of each scheme's potential and neglect several influential aspects such as the effect of spring-neap conditions, the implications of intertidal regions and the footprint of the structures on tidal hydrodynamics.

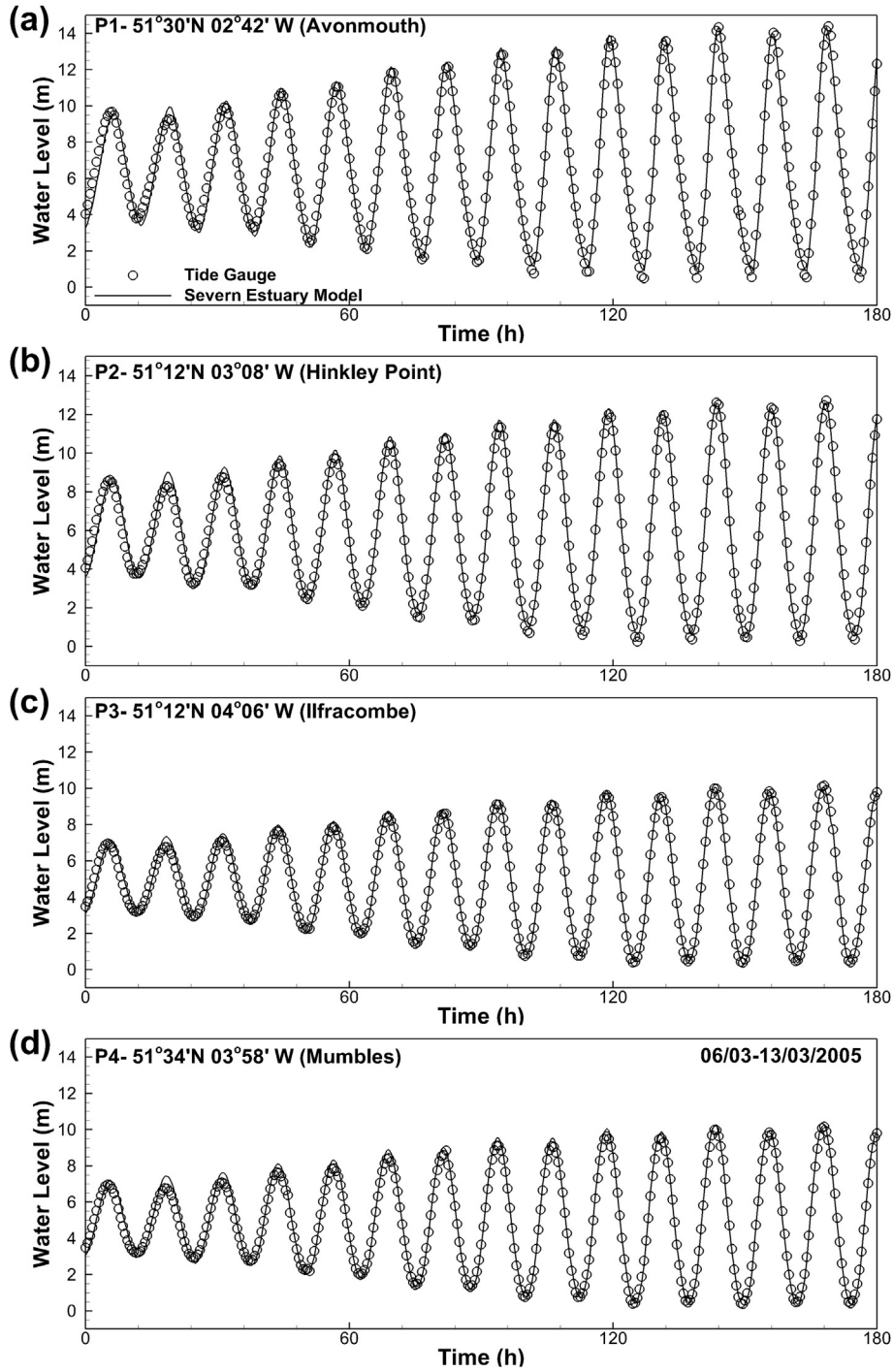


Fig. 3. Comparison between predicted and measured water level data, observed through the UK Tide Gauge Network.

Table 2
Potential Energy and Annual Energy output estimates for the tidal impoundments based on [25].

| Tidal range power plants | Impounded area A (km ²) | Mean amplitude h _a (m) | Annual potential energy E _{max_yr} (TWh/yr) | Ebb generation output estimate (TWh/yr) | Two-way generation output estimate (TWh/yr) |
|---------------------------|-------------------------------------|-----------------------------------|--|---|---|
| Swansea Bay Lagoon (SBL) | 11.6 | 3.29 | 0.99 | 0.27 | 0.37 |
| Cardiff Lagoon (CL) | 65 | 4.31 | 9.50 | 2.57 | 3.52 |
| Newport Lagoon (NL) | 32 | 4.43 | 4.96 | 1.34 | 1.83 |
| Severn Barrage (STPG/HRC) | 573 | 4.24 | 81.24 | 21.93 | 30.06 |

Table 3
Tidal turbine specifications.

| Turbine Parameters | Tidal range power plants | | |
|---|--------------------------|-------------------------|-------------------------|
| | Swansea bay Lagoon | Cardiff/Newport lagoons | Severn barrage stpg/hrc |
| Turbine Capacity (MW) | 20 | 30 | 40 |
| Generator Poles G_p | 97 | 113 | 142 |
| Turbine Diameter D (m) | 7.35 | 8.90 | 9.00 |
| Fluid Density ρ (kg/m ³) | 1025 | 1025 | 1025 |
| Turbine Speed S_p | 61.9 | 53.9 | 42.3 |
| Electricity Grid Frequency f_g (Hz) | 50 | 50 | 50 |

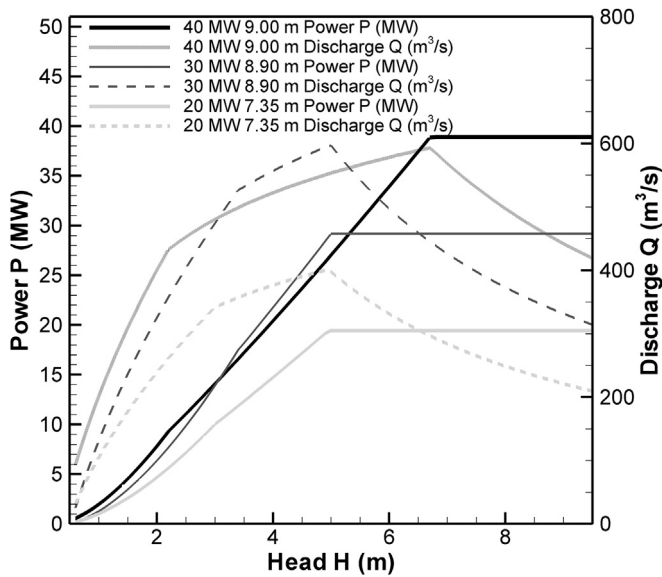


Fig. 4. Turbine hill charts used for: (a) Swansea Bay Lagoon (20 MW), (b) Cardiff and Newport Lagoons (30 MW) and (c) the Severn Barrage designs (40 MW).

The impoundment shape in each case is the product of a host of parameters that include geomorphological characteristics to allow the embankment and hydraulic structure construction, established shipping lanes, socio-economic activities and environmental aspects, such as river outflows, fish population movement etc. Therefore, further altering the impoundment shape was not considered here. Instead, the configuration for the STPG Severn Barrage was adopted from available data [44,47]. Similarly, the Swansea Bay lagoon was defined according to information provided from the Development Consent Order application of the project [34] and [24]. For the more recent Cardiff and Newport lagoons, data were obtained from associated technical reports [35], company presentations and communications. Given information for turbine specifications of each project (Table 3) were fed into equations (3)–(8) to produce the hill charts of Fig. 4 linking H with the turbine flow-rate Q and the generated power P .

A preliminary 0-D optimisation study was conducted using as input tidal predictions from the Severn Estuary model (such as Fig. 3). For the more developed proposals of the STPG scheme and the Swansea Bay Lagoon, this was focused on identifying suitable specifications (e.g. h_{st} , t_h) for the sequences given in Fig. 1 and Table 1. For the Cardiff and Newport lagoons, due to the early stage of these proposals, it was first necessary to also establish an appropriate number of turbines and sluice gates, taking into account the impounded surface area, the intertidal regions, hydraulic structure specifications and the respective limitations as discussed in Ref. [6]. A modified design for the Severn Barrage was also assessed, hereinafter referred to as Severn Barrage HRC (Hydro-

environmental Research Centre), with more turbines distributed across the structure, aiming for a superior two-way operation performance, subject to constraints such as: bathymetry, caisson size and the allocated space for ship locks and substations. The HRC barrage is introduced here to facilitate a comparison with the more up-to-date proposals that opt for a two-way, rather than ebb-only, generation, while maintaining the same turbine technology as the earlier barrage for consistency. The converged specifications for the hydrodynamic modelling investigation are summarised in Tables 4 and 5. The project information of Table 4 demonstrates how the scale of tidal power proposals in the Bristol Channel and Severn Estuary varies in terms of the installed capacity and impoundment length.

Five numerical model layouts were developed with their meshes being refined around the hydraulic structure configurations, as illustrated in Fig. 5. The Severn Barrages (STPG and HRC) and the Swansea Bay Lagoon (SBL) were modelled individually, i.e. simulations 2-D-STPG, 2-D-HRC and 2-D-SBL respectively. The Cardiff Lagoon (CL) was only modelled to operate in conjunction with the SBL scheme (2D-SBL,CL) as the proposal would only progress once the first lagoon is already in place. Similarly, the Newport Lagoon would follow the CL scheme, and therefore the simulation 2-D-SBL,CL,NL encompasses all three lagoons simultaneously, providing an insight into the cumulative impact of all the lagoons.

The numerical models were run under three different sequences and for the same tidal conditions, to examine the effects of the operation of the various schemes on the hydrodynamics and energy output. These were:

- An ebb-only operation (EO) with specifications $h_{st} = 4.0$ m, $h_{min} = 1.0$ m and $t_h = 2.2$ h (parameters defined in Table 1) for all projects,
- An optimised two-way operation (TW1) where each impoundment adopts the optimum specifications of Table 5 to maximise energy output, and
- A conservative two-way operation (TW2) with $h_{st} = 2.5$ m, $h_{min} = 1.0$ m that aims for an increased generation time through a reduced maximum holding time of $t_h = 1.5$ h.

4. Results and discussion

The hydrodynamic model results were analysed to assess two characteristics of the tidal power plant operation. Firstly, the effects on the regional tidal flow for each scheme are investigated. In turn, the annual energy produced from the ebb-only and two-way scenarios contemplated (EO, TW1 and TW2) is evaluated.

4.1. Hydrodynamic impact

Flow patterns of interest can be identified from the instantaneous plots in Fig. 6 for the tidal lagoons during spring ebb (top row) and flood (bottom row) tides. For ebb generation, the lagoon turbine sections are orientated according to the receding flow

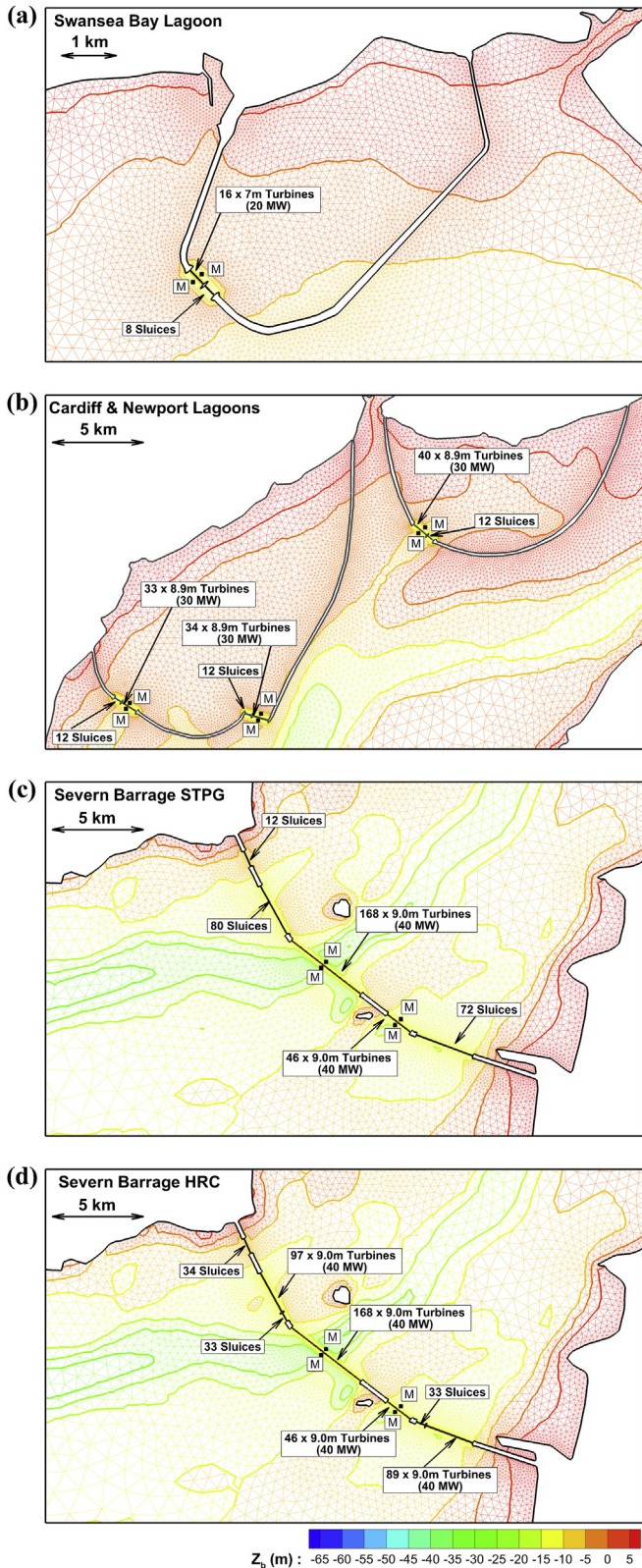


Fig. 5. Computational domains and tidal power plant configuration for: (a) Swansea Bay Lagoon design, (b) Cardiff and Newport Lagoons configurations, (c) Severn Barrage [31] configuration, and (d) modified Severn Barrage HRC configuration designed for two-way generation. Water level Monitor points (M) in close proximity to turbine sections used for the assessment of hydrodynamic impacts are also indicated.

direction, as suggested by the predicted streamlines in the top row of Fig. 6. During flood generation, the water jets induced by the turbines correspond to the development of large counter-rotating vortices upstream (Fig. 6). These recirculation zones expand as the momentum of the water jets dissipate, due to the gradual decrease in the water head difference across the hydraulic structures. At holding periods the vortices (or eddies) subsequently tend to occupy a large proportion of the impounded area. In contrast to the high velocity currents during flood tides, the velocity magnitudes upstream of the structures during ebb tides away from the hydraulic structures are consistently weaker. Therefore, it is speculated that the upstream ebb currents will be unable to flush out sediments accumulated during the flood tide.

A similar pattern emerges with the STPG Barrage, while operating under an ebb-only sequence (Fig. 7a, left). Vortices and stagnant regions prevail downstream as the turbines are concentrated only in the middle third of the impoundment and flow is restricted from the adjacent sluice gates at this stage. With the introduction of turbines in the HRC scheme, which replace parts of the sluice gates (Fig. 5c–d), these effects are largely mitigated (Fig. 7a, right). For flood tides, the STPG barrage would operate in the filling mode (Table 1), while the HRC is generating (Fig. 7b). In both cases, the wide distribution of hydraulic structures over the impoundment length allows a flow direction that is almost consistent with the status quo as long as all of the hydraulic structures (i.e. turbines and sluices) are open.

The formation of recirculation zones can be detrimental environmentally since scalars (e.g. suspended sediments and pollutants) will be drawn to the centroid of the vortices by the imbalance between the centrifugal force and bed friction. As a consequence of the stagnant flow in the centre, and mainly near the bed, sediments can settle over time and result in rapid geomorphological changes. Apart from distributing the hydraulic structures (Fig. 7b), a more feasible alternative to addressing this complex hydrodynamic process would be to position sluice gates in such a manner that targets their wake through the recirculation centroid, dissipating the vorticity as much as possible. For the case of the STPG barrage, this approach could be applicable at ebb tide by opening the sluice gates as soon as the head difference restricts generation from the turbines. The characteristics of sediment transport in particular within the Severn Estuary have been well documented [21,22,38]. As a result, these hydrodynamic patterns developed in both lagoons and barrages should be further studied for their implications for sediment deposition. Otherwise, the preservation of the upstream geomorphology may require regular dredging operations over the project lifetime [23]; [15].

The hydrodynamic impacts of tidal impoundments extend beyond the flow patterns close to the turbine and sluice regions (Figs. 6 and 7). It has been shown that for ebb-only operation, the STPG Barrage would affect water levels and current velocities as far as the Irish Sea [11,47,48]. However, these can otherwise be largely confined to the Bristol Channel, subject to a two-way operation and an optimised regulation of turbines and sluices over spring-neap tidal conditions [49].

The contour plots of Fig. 8 examine the implications of tidal lagoons and the HRC Barrage, all operated under the TW2 specifications. A Swansea Bay lagoon on its own (Fig. 8a) has a negligible impact on the hydrodynamic characteristics in the Bristol Channel due to its relatively small size. The lagoon footprint is contained primarily within the Swansea Bay region and features flow accelerations in areas affected by turbine and sluice gate wakes. On the upstream side, a reduction by approximately 0.65 m in maximum water levels and an increase of 0.35 m in minimum water levels was predicted, which is an expected characteristic of a two-way generation scheme (Fig. 1).

Table 4
Tidal range energy project case studies specifications.

| Specifications | Tidal range power plants | | | | |
|---|--------------------------|---------------------|---------------------|-----------------------|----------------------|
| | Swansea bay Lagoon (SBL) | Cardiff Lagoon (CL) | Newport Lagoon (NL) | Severn barrage (STPG) | Severn barrage (HRC) |
| Turbine Number | 16 | 67 | 40 | 216 | 400 |
| Turbine Capacity (MW) | 20 | 30 | 30 | 40 | 40 |
| Turbine Diameter (m) | 7.35 | 8.9 | 8.9 | 9.0 | 9.0 |
| Turbine Flow Area (m ²) | 679 | 4168 | 2488 | 13,741 | 25,447 |
| Sluice Flow Area (m ²) | 800 | 2400 | 1200 | 35,000 | 10,000 |
| Total Capacity (MW) | 320 | 2010 | 1200 | 8640 | 16,000 |
| Length of Impoundment (km) | 9.6 | 20.8 | 16.4 | 16.1 | 16.1 |
| Primary Operational Sequence Considered | Two-Way | Two-Way | Two-Way | Ebb | Two-Way |

Table 5
Operation specifications for two-way operation following a 0-D optimisation study for maximum power output.

| Tidal range power plants | Generation starting head | Minimum generation head | Maximum holding duration | Annual 0-D energy generated |
|--------------------------|--------------------------|-------------------------|--------------------------|-----------------------------|
| | h_{st} (m) | h_{min} (m) | t_h (h) | E (TWh/yr) |
| Swansea Bay Lagoon (SBL) | 4.10 | 1.00 | 3.80 | 0.615 |
| Cardiff Lagoon (CL) | 4.50 | 1.00 | 3.60 | 5.28 |
| Newport Lagoon (NL) | 4.70 | 1.00 | 3.80 | 3.05 |
| Severn Barrage (STPG) | 2.50 | 1.00 | 1.50 | 25.01 |
| Severn Barrage (HRC) | 3.60 | 1.00 | 2.50 | 36.06 |

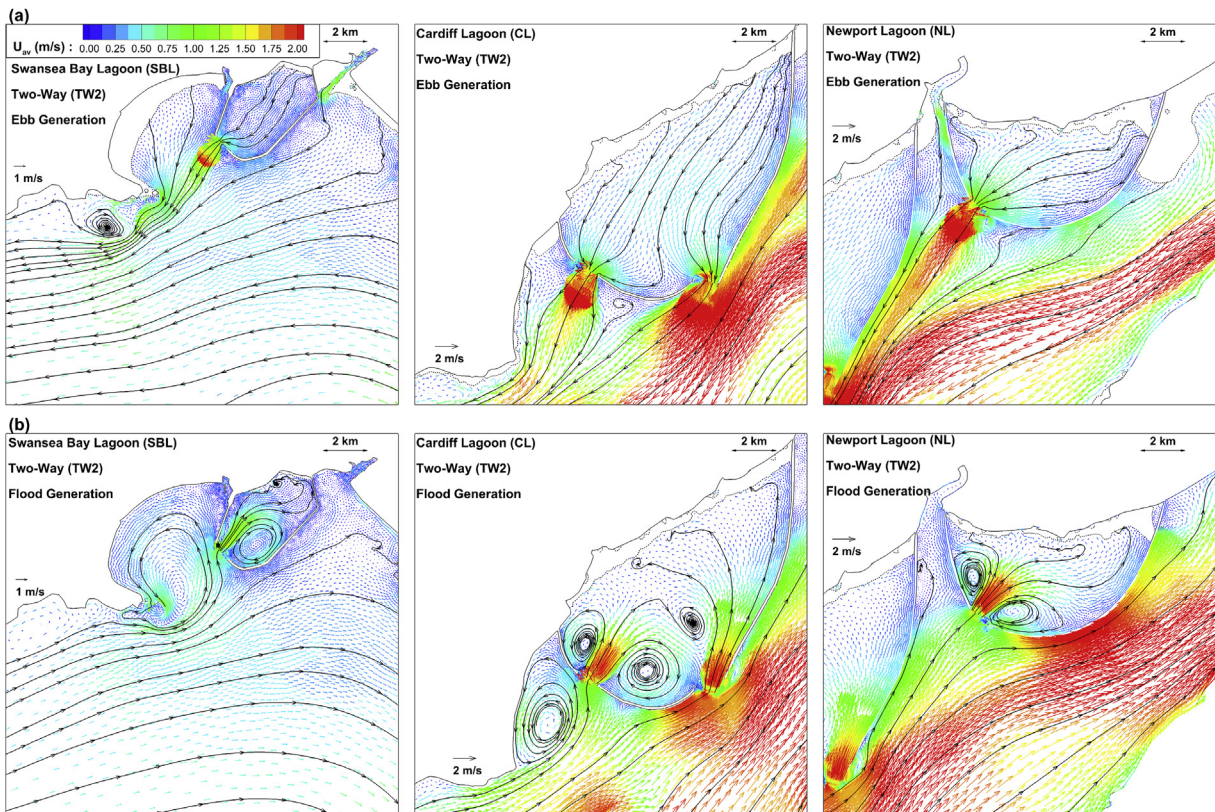


Fig. 6. Instantaneous streamlines and velocity vectors during ebb and flood tides following the introduction of tidal energy lagoons.

As the scale of the projects increases, so do the relative hydrodynamic impacts. Once the Cardiff Lagoon is introduced, current accelerations can be observed along the main Severn Estuary channel (Fig. 8b). In contrast, the maximum current velocity upstream of the Cardiff impoundment is markedly reduced within the majority of the impounded area. Implications for the water level maxima present themselves far-field, with increases surpassing the

0.05 m contour threshold in parts of the Bristol Channel. The operation of all three lagoons simultaneously (Fig. 8c) features a reduction in the maximum water levels of the order of 0.25 m within the estuary during high spring tides, primarily due to the influence of the structures on the estuarine tidal resonance. This is accompanied with an increase of approximately 0.1 m in the Swansea Bay region, indicating a cumulative hydrodynamic impact

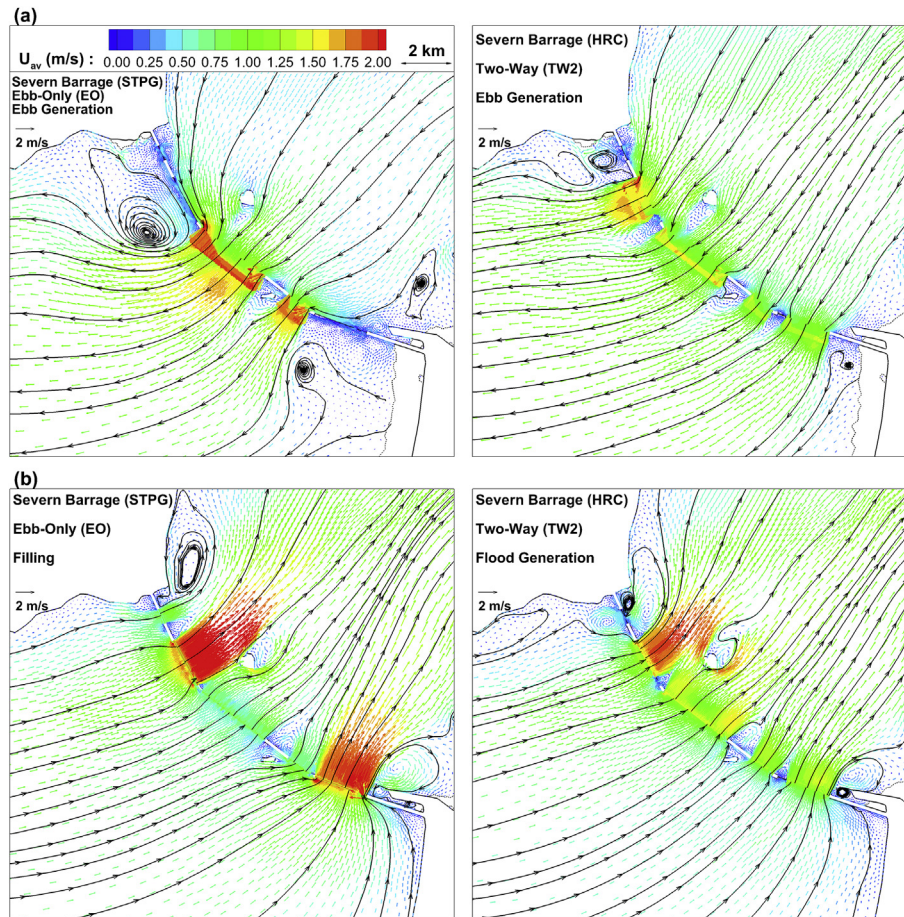


Fig. 7. Instantaneous streamlines and velocity vectors during: (a) ebb and (b) flood tides for the ebb-only Severn Barrage (STPG) and the modified Severn Barrage (HRC) designed for two-way operation.

when developing multiple lagoons in close proximity. Nonetheless, the combined effects of the lagoons are still noticeably less than the comparable effects of an HRC barrage (Fig. 8d). Specifically, the barrage features an increase of the maximum water levels at Swansea Bay by around 0.3–0.4 m and a decrease by up to approximately 4.0 m close to Avonmouth during high spring tides. However, these values are heavily dependent upon the operational sequence and could be improved in all cases following developments in turbine technologies focused on expanding their versatility over generating head differences and pumping possibilities.

In turn, Fig. 9 demonstrates how the operational procedures can also be accountable for far-field and near-field hydrodynamic impacts. Taking simulation 2-D-SBL, CL, NL as an example, an ebb-only sequence (EO) influences conditions downstream differently from the TW2 operation (Fig. 8c). Maximum water levels upstream are better preserved at the expense of a greater difference in minimum water levels (Fig. 9a). The effects of an optimised two-way operation for power output (TW1) similarly correspond to deviant results from TW2 (Fig. 8c) demonstrating the importance of appropriate parameter selection (i.e. t_h and h_{st}). Indicatively, for the upstream monitoring points in Fig. 9, a TW2 sequence corresponds to maximum water level reductions of approximately 0.7, 2.1 and 1.6 m for SBL, CL and NL respectively.

A more quantitative assessment on the hydro-environment footprint is feasible through the introduction of the indicators in Table 6. For downstream conditions, the RMSD value from the Mean Water Levels (MWL) was calculated with and without the

impoundments in the numerical models at the downstream monitor points indicated in Fig. 5. The influence of the Swansea Bay lagoon appears insignificant as it changes from an RMSD of 2.22 m before construction to 2.20–2.21 m after. The greatest effect on tidal levels is reflected by the STPG Barrage under a two-way sequence due to the opening of the sluice gates ($A_{sl_STPG} = 35,000 \text{ m}^2$) for a water head difference of ≈ 1.0 m between modes 3–4 and 7–8 (Table 1). The heightened momentum flow through these hydraulic structures generates instantaneous perturbations despite their gradual opening represented numerically using ramp functions for a smoother transition. The RMSD value is altered from 2.79 to 1.97 m, i.e. by 0.82 m. For the HRC variant on the other hand, the modified configuration corresponds to a reduction by 0.35 m on the RMSD, indicating less interference.

With regards to upstream conditions, three indicators are introduced. The first one calculates changes to the upstream MWL in m at the monitoring points directly upstream of the turbine sections illustrated in Fig. 5. Under an ebb-only operation (EO), the MWL increases. Such changes can relate to local groundwater levels and, in turn, threaten adjacent vulnerable communities to flooding. For two-way sequences (TW1, TW2) this indicator is redundant as it remains unaltered as long as appropriate specifications have been imposed (Table 4). The second indicator refers to the quantification of the upstream tidal range lost at the monitoring points shown in Fig. 5. The minimum change is predicted for the Swansea Bay lagoon with a value of 14% while operating under TW2. In contrast, the greatest reduction is presented by the barrage (41% -STPG EO) which could be reduced (to 30% -HRC EO) if the design is optimised.

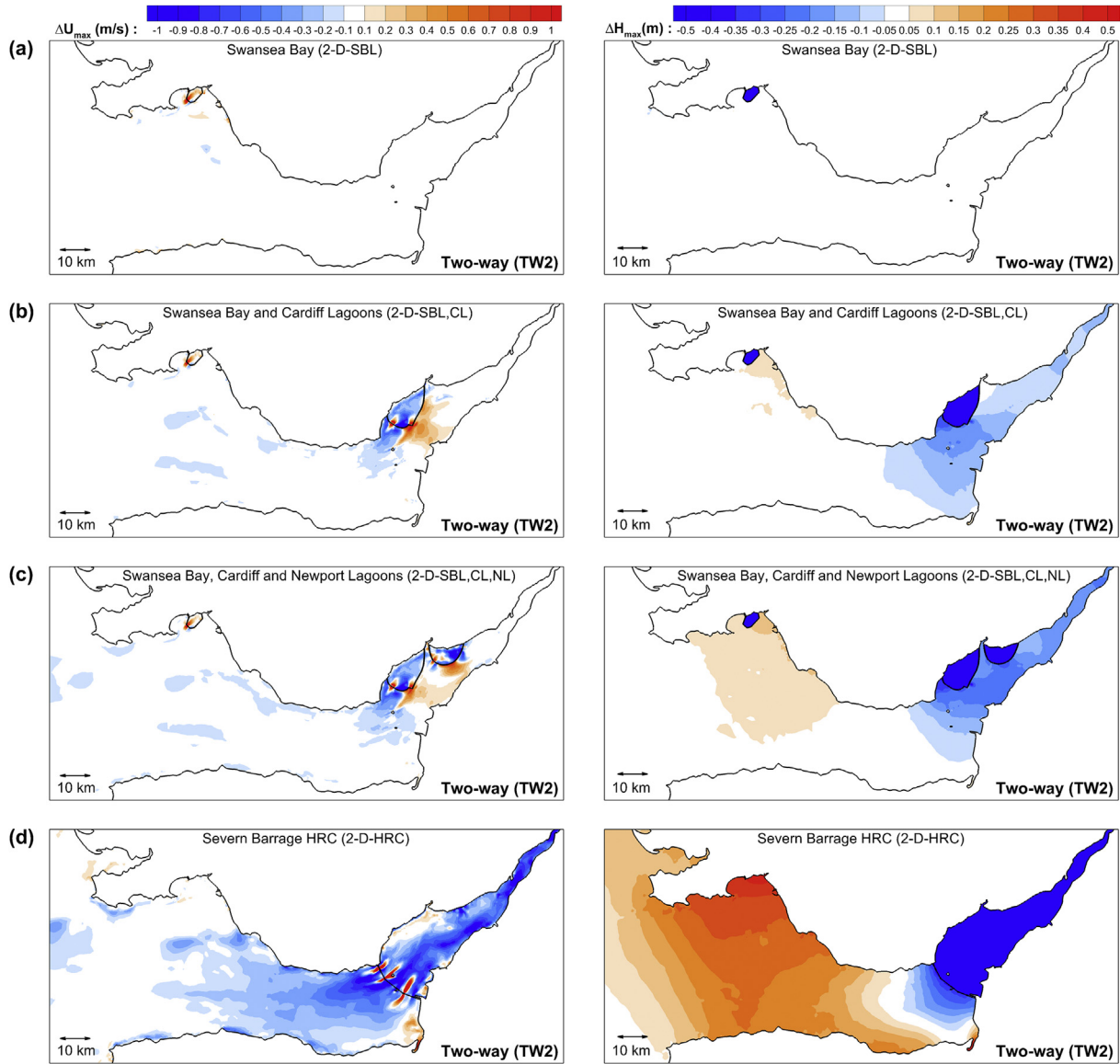


Fig. 8. Cumulative Impact of Tidal Lagoons and the Severn Barrage HRC on maximum velocities (left column) and maximum water levels (right column) under the TW2 operation sequence.

The intertidal area loss is also of interest and appears to be closely linked with the operational sequence and was calculated by comparing the area subjected to wetting and drying before and after the introduction of the tidal power plants. EO corresponds to significant losses, which range from 24 to 50%. In contrast, the more balanced TW2 minimises this loss to 14–22%, illustrating how a careful regulation of the turbines and sluice gates can effectively mitigate environmental issues associated with the proposed tidal range power plants.

4.2. Annual energy potential

A critical aspect motivating the consideration of tidal power plants is the annual energy produced for the various schemes post-construction. For this assessment, simulations were undertaken for spring-neap cycles over a lunar month period (≈ 29.53 days), based on the specifications given in Tables 3 and 4. The manner in which energy is generated from the tidal power plants is the focus of Fig. 10, which demonstrates the power generated over a simulation

time of 180 h and during a transition period from neap to spring tide conditions. A lower energy production is calculated for neap tides, which gradually increases proportionally with the amplitude at spring tides. For the tidal lagoons operating under the same sequence (TW2) in Fig. 10a, the power generation intermittency is shared since the phase of the tides does not change substantially within the Bristol Channel and the Severn Estuary. In Fig. 10b, the power generation output from an ebb-only (EO) STPG barrage is plotted against the two-way (TW2) HRC barrage, highlighting the significance of the sequence and the impoundment design on harnessing power from the same resource.

A large fraction of the generation gaps in Fig. 10 could be filled through either potential tidal stream arrays or other tidal impoundments developed in areas of a different tidal phase, such as along the North Wales coast [6] and in the Irish Sea [3,36]. Alternatively, introducing turbine pumping on the operational sequence in the presence of multiple projects could provide some flexibility on the generation time, as well as net energy gains [37]. Unfortunately, opportunities presented by tidal turbine pumping have

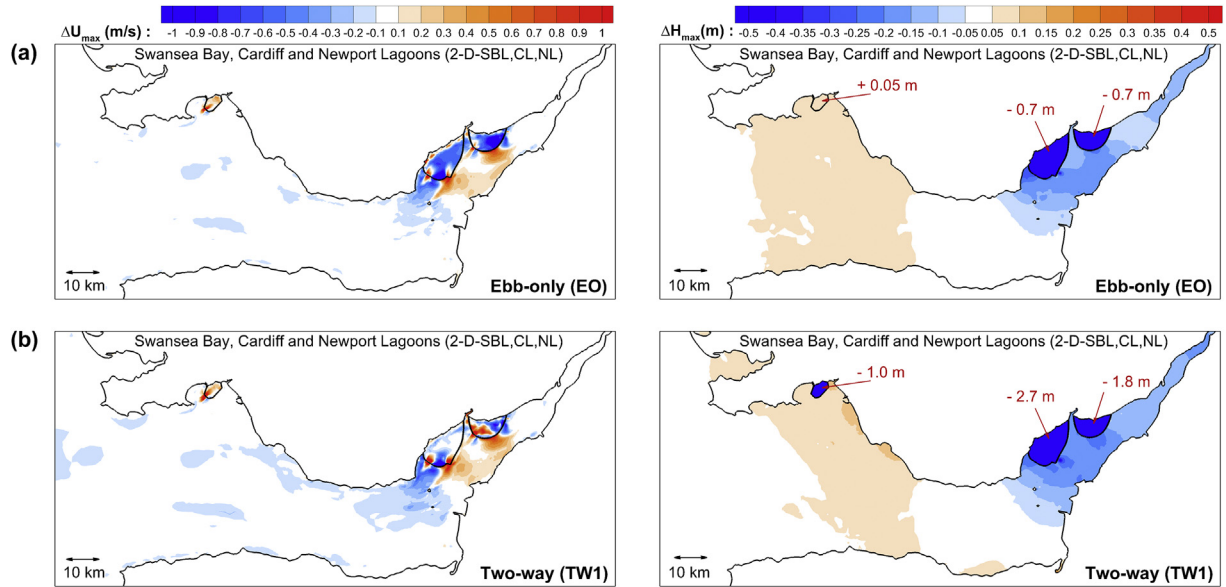


Fig. 9. Operation sequence effect on maximum velocity (left column) and water levels (right column) regionally: (a) Ebb-only (EO) and (b) Two-way (TW1).

Table 6
Implications of different operational sequences and specifications on regional tidal conditions and plant performance according to simulations 2D-SBL, CL, NL, 2-D-STPG and 2-D-HRC. Descriptions and values in italics refer to the established conditions, i.e. in the absence of tidal lagoons or barrages at the respective sites.

| Operation impacts | Operation sequence | Tidal power plants | | | | |
|--|--------------------|--------------------------|---------------------|---------------------|----------------------|---------------------|
| | | Swansea bay Lagoon (SBL) | Cardiff Lagoon (CL) | Newport Lagoon (NL) | Sewer barrage (STPG) | Sewer barrage (HRC) |
| <i>RMSD of Water Levels from MWL (m)</i> | - | 2.22 | 2.89 | 2.97 | 2.79 | 2.79 |
| <i>RMSD of downstream Water Levels from M.W.L. (m)</i> | EO | 2.20 | 2.79 | 2.84 | 2.44 | 2.47 |
| | TW1 | 2.20 | 2.78 | 2.82 | 1.97 | 2.44 |
| | TW2 | 2.21 | 2.81 | 2.88 | 1.97 | 2.48 |
| <i>MWL according to Ordnance Datum(m)</i> | - | 0 | 0 | 0 | 0 | 0 |
| <i>Upstream Mean Water Level change (m)</i> | EO | 0.84 | 1.06 | 0.94 | 2.36 | 0.96 |
| | TW1 | 0.05 | -0.01 | -0.19 | 0.09 | -0.01 |
| | TW2 | 0.03 | 0.02 | -0.06 | 0.09 | 0.01 |
| <i>Maximum Tidal Range predicted (m)</i> | - | 10.55 | 13.82 | 14.35 | 13.45 | 13.45 |
| <i>Upstream Tidal Range Reduction (%)</i> | EO | 14% | 17% | 15% | 41% | 30% |
| | TW1 | 16% | 23% | 26% | 38% | 33% |
| | TW2 | 14% | 17% | 20% | 38% | 31% |
| <i>Intertidal area at the proposed region (km²)</i> | - | 4.6 | 20.4 | 22.7 | 237.0 | 237.0 |
| <i>Intertidal area Loss (%)</i> | EO | 50% | 42% | 47% | 34% | 24% |
| | TW1 | 24% | 18% | 27% | 22% | 17% |
| | TW2 | 20% | 14% | 22% | 22% | 15% |
| <i>Power Generation time per year (%)</i> | - | 0% | 0% | 0% | 0% | 0% |
| <i>Power Generation time per year (%)</i> | EO | 38% | 34% | 34% | 51% | 38% |
| | TW1 | 47% | 54% | 54% | 73% | 62% |
| | TW2 | 63% | 70% | 70% | 73% | 69% |

been limited (e.g. La Rance barrage) due to the pumping efficiency, substantial energy storage and electricity grid infrastructure required to support such functions. Pumping has consequently not been considered in the sequences of Fig. 1, but does invariably promise future dimensions to dynamically adjust the operation and match more efficiently the energy demands of the electricity grid.

The energy output results were extrapolated to a yearly period (≈ 365 days) and are summarised in Table 7 for each plant and operational sequence (EO, TW1 and TW2). It is noted that these extrapolations are tailored to the particular spring-neap water level input used over the lunar period and therefore the annual energy output could be influenced by the varying tidal conditions developed over the rest of the year. Nonetheless, the boundary conditions over the two same spring-neap tidal cycles were deemed sufficient for representative and comparative results. As expected,

the optimised specifications associated with TW1 (Table 5) correspond to the highest energy yield, followed by the more generic TW2 and finally EO. An exception to this rule is the STPG barrage, which performs better under an ebb-only rather than a two-way operation in terms of its energy output. This is aligned with findings reported from previous studies of the STPG scheme [45].

Preliminary estimates from a refined 0-D modelling tool [6] are provided (Fig. 10 and Table 7) as a benchmark of how much energy can be generated if the hydrodynamic influences are neglected. The manner in which 0-D models overestimate energy levels can be appreciated in Fig. 10 where results are plotted along with the outputs from hydrodynamic models. Deviations are attributed mainly to (a) the 0-D model inability to capture the effects of the pronounced flowrates through turbines and sluices on the Water head differences that dictate the instantaneous power output and

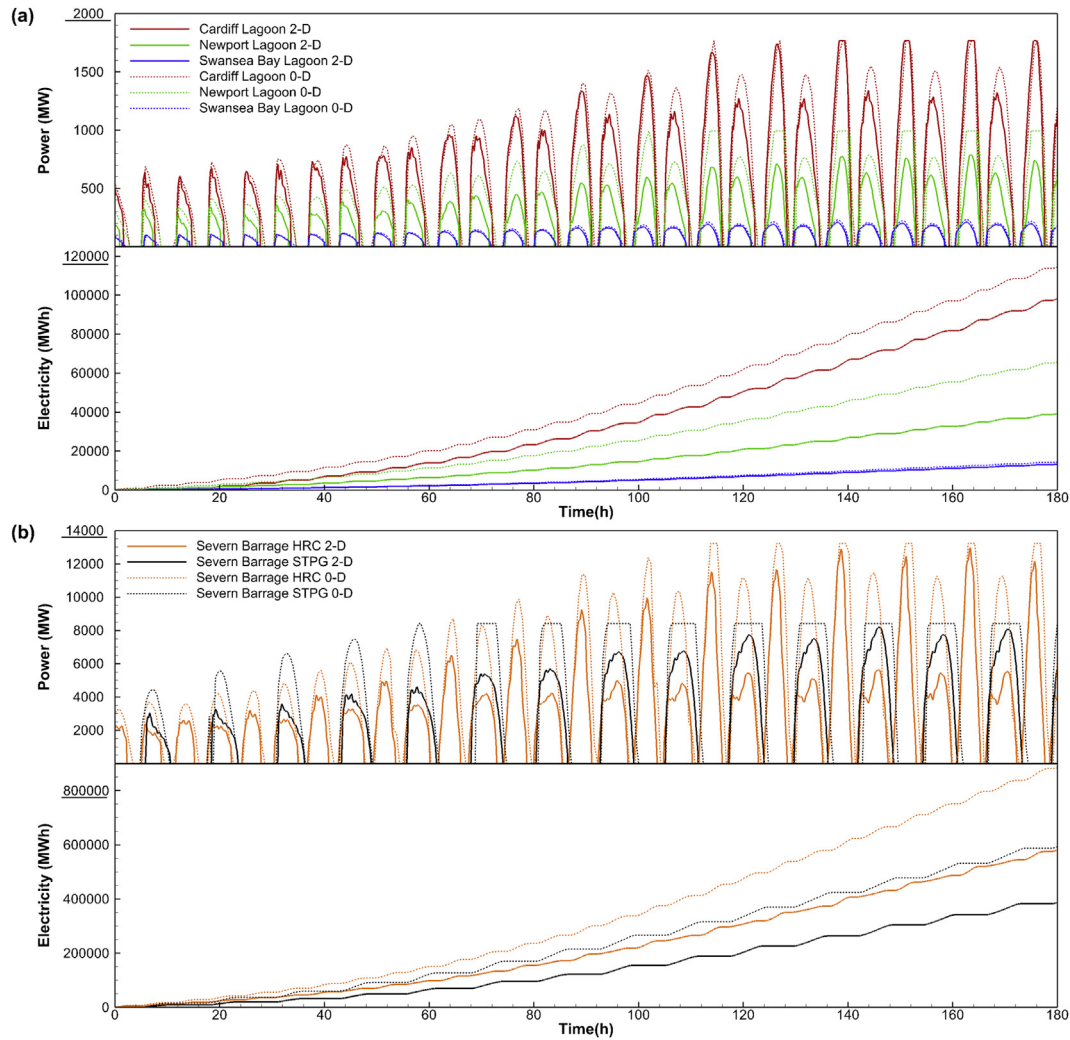


Fig. 10. Power Generation and cumulative energy over the transition from neap to spring tides according to the 0-D and 2-D models for: (a) the combined Swansea Bay, Cardiff and Newport lagoon operation and (b) the ebb-only Severn Barrage (STPG) and the modified version for two-way generation (HRC).

(b) the difficulty to accurately parametrising 2-D and 3-D effects such as wetting and drying through a simplified function of water level variations against surface area. With a combination of all three tidal lagoons 0-D estimates suggest that 8.95 TWh/yr can be harnessed under TW1, which would at present cover approximately 2.8% of the UK's annual electricity needs (≈ 323 TWh/yr). On the other hand, this percentage is decreased to 2.3% (7.37 TWh/yr) based on 2-D modelling (2-D-SBL, CL, NL), that gives a 17.5% loss due to regional hydrodynamic impacts. This is even more pronounced for the HRC Barrage, where 0-D results estimate a production of more than 11.2% (36.06 TWh/yr) of the UK's current energy needs, with the 2-D model yielding 6.8% (22.05 TWh/yr). This represents a more substantial 38.9% loss in energy through greater hydrodynamic effects (Fig. 8d). Nonetheless, an HRC Barrage could produce approximately three times the energy of the combined tidal lagoons.

Earlier studies adopting a 0-D modelling approach for the Swansea Bay Lagoon predicted 0.478 and 0.596 TWh/yr for two-way and ebb-only generation respectively [24]. Equivalent values estimated here were 0.315, 0.615 and 0.507 TWh/yr for EO, TW1 and TW2 respectively. However, the more accurate 2-D-SBL model results correspond to 0.292, 0.586 and 0.474 TWh/yr for the Swansea Bay lagoon, closely matching the current value quoted by TLP of 0.495 TWh/yr [35] for two-way operation.

The Cardiff Lagoon impounds 5.6 times the area of the Swansea Bay Lagoon (Table 2), but produces ≈ 8 times the energy. The energy output is enhanced relatively to the impounded area due to the tidal resonance and advective flow effects that facilitate greater H differences over the tidal cycle within the estuary. On the other hand, as additional lagoons are introduced regionally, the performance of individual lagoons is undermined due to their cumulative hydrodynamic impacts (Fig. 8b–c). In the simulations, for both the Swansea Bay and Cardiff lagoons (2-D-SBL,CL), additional losses are reported for SBL (Table 7) attributed to the influence of the larger lagoon. It can be observed in Fig. 8b how the presence of the Cardiff Lagoon affects the water levels and velocity maxima beyond the Severn Estuary and even as far as Swansea Bay. The combination of the three lagoons further accentuates these interactions and features a substantially lower energy output by as much as 30.5% (Table 7) for the Newport lagoon. This deviation compared to the 0-D results is not only accredited to the lagoon interactions, but also to the more comprehensive manner intertidal areas are represented in the 2-D model. It is therefore demonstrated how a 0-D modelling approach can substantially overestimate the potential of schemes featuring both large intertidal regions (e.g. Newport Lagoon) and the upstream surface area (e.g. the Severn Barrages).

Table 7

Annual energy results for the tidal range structures in the Severn Estuary and Bristol Channel under the EO, TW1 and TW2 operational sequences.

| Numerical simulations | Tidal range project annual energy (TWh/yr) | | | | | Hydrodynamic impact (%) ^a | | | | | Total energy (TWh/yr) |
|---|--|---------------------|---------------------|-----------------------|----------------------|--------------------------------------|-------|-------|-------|-------|-----------------------|
| | Swansea bay Lagoon (SBL) | Cardiff Lagoon (CL) | Newport Lagoon (NL) | Severn barrage (STPG) | Severn barrage (HRC) | SBL | CL | NL | STPG | HRC | |
| <i>EO: Ebb Generation: $h_{st} = 4.0m$, $h_{min} = 1.0m$, $t_h = 2.2 h$</i> | | | | | | | | | | | |
| 0-D | 0.315 | 3.07 | 1.57 | 23.03 | 23.01 | – | – | – | – | – | – |
| 2-D – SBL | 0.292 | – | – | – | – | –7.3 | – | – | – | – | 0.29 |
| 2-D – SBL,CL | 0.291 | 2.89 | – | – | – | –7.6 | –5.9 | – | – | – | 3.18 |
| 2-D – SBL,CL,NL | 0.290 | 2.77 | 1.25 | – | – | –7.9 | –9.8 | –20.4 | – | – | 4.31 |
| 2-D – STPG | – | – | – | 15.77 | – | – | – | – | –31.5 | – | 15.77 |
| 2-D – HRC | – | – | – | – | 16.35 | – | – | – | – | –28.9 | 16.35 |
| <i>TW1: Two-way generation (1) – Max Power: Specifications of Table 5</i> | | | | | | | | | | | |
| 0-D | 0.615 | 5.28 | 3.05 | 25.01 | 36.06 | – | – | – | – | – | – |
| 2-D – SBL | 0.586 | – | – | – | – | –4.8 | – | – | – | – | 0.59 |
| 2-D – SBL,CL | 0.577 | 4.68 | – | – | – | –6.2 | –11.4 | – | – | – | 5.26 |
| 2-D – SBL,CL,NL | 0.575 | 4.55 | 2.25 | – | – | –6.5 | –13.9 | –26.3 | – | – | 7.37 |
| 2-D – STPG | – | – | – | 15.31 | – | – | – | – | –38.8 | – | 15.31 |
| 2-D – HRC | – | – | – | – | 22.05 | – | – | – | – | –38.9 | 22.05 |
| <i>TW2: Two-way generation (2) – Reduced holding time:: $h_{st} = 2.5 m$, $h_{min} = 1.0m$, $t_h = 1.5 h$,</i> | | | | | | | | | | | |
| 0-D | 0.507 | 4.37 | 2.49 | 25.01 | 33.76 | – | – | – | – | – | – |
| 2-D – SBL | 0.474 | – | – | – | – | –6.5 | – | – | – | – | 0.47 |
| 2-D – SBL,CL | 0.464 | 3.94 | – | – | – | –8.5 | –9.9 | – | – | – | 4.40 |
| 2-D – SBL,CL,NL | 0.462 | 3.87 | 1.73 | – | – | –8.9 | –11.4 | –30.5 | – | – | 6.06 |
| 2-D – STPG | – | – | – | 15.31 | – | – | – | – | –38.8 | – | 15.31 |
| 2-D – HRC | – | – | – | – | 21.53 | – | – | – | – | –36.2 | 21.53 |

^a The hydrodynamic impact refers to the deviation from 0-D annual energy results which discount the tidal impoundment impact on the hydro-environment.

5. Conclusions

Details have been provided on the refinement and application of a two-dimensional hydrodynamic model for the assessment of tidal range structure operations. Following preliminary optimisation and validation studies, the model was employed to assess a number of tidal barrage and lagoon proposals within the Severn Estuary and Bristol Channel, in the UK.

Tidal lagoons generally have less of an overall environmental impact than previous tidal range structure proposals in the region. However, there are still noticeable alterations to the estuary hydrodynamics, with local advective accelerations and turbulent wakes close to the turbine/sluice sections, and flow stagnation upstream of the lagoons leading to the creation of pronounced recirculation zones. Lagoons in the Severn Estuary lead to increased currents in the channel reaches passing the lagoon, which will inevitably lead to increased turbidity in the region. Some implications on the tidal level maxima are reported, with relative reductions in the Severn Estuary and increases in the levels in the Bristol Channel. The barrage options featured more pronounced hydro-environmental impacts, but a more significant annual energy production. Pumping has not been considered in the studies reported herein, but if introduced at low and high water it could reduce the degree of hydro-environmental change.

It was considered that predictions can vary according to the power plant operation over time, and therefore specifications were converged through optimisation analyses for ebb-only and two-way operational sequences. The combined potential of the lagoons has been predicted from model simulations to produce approximately 2.3% of current UK electricity needs from the Swansea Bay, Cardiff and Newport lagoons respectively. In contrast, a modified Cardiff-Weston barrage for two-way generation could produce from the same region approximately three times the energy yield (i.e. 6.8% of current UK electricity needs).

Certain implications can be drawn with regards to tidal range structures from the analysis. As with other types of marine renewable energy platforms (e.g. wave energy converters and tidal stream technologies), tidal barrages and lagoons are similarly

subject to co-location issues. Addressing the interactions which correspond to detrimental impacts on the performance of individual schemes will be critical for the success of this tidal energy industry. For example, adopting different operational sequences for each scheme to enable nearby lagoons to generate at different times may reduce these losses. However, it is shown that ebb-only or flood-only generation sequences will have their respective implications, such as greater intertidal area losses and far-field effects. Therefore, variable operational sequences and specifications should be tested to facilitate an efficient performance that takes into account both individual and surrounding renewable energy platforms, as well as their hydro-environmental impacts. Consequently, it might be advantageous to opt for an operation that prefers a more conservative approach on the grounds of minimising power generation intermittency and hydrodynamic impacts, instead of one that has been exclusively optimised to maximise annual energy production but features more adverse effects.

Acknowledgements

The authors acknowledge the support through the MAREN2 project, part funded by the European Regional Development Fund (ERDF) through the Atlantic Area Transnational Programme (INTERREG) under contract No. 2013-1/225, during which parts of the numerical model were developed. The authors would also like to express their gratitude to Prof Chris Binnie for his insightful comments over the course of this research.

References

- [1] T.A.A. Adcock, S. Draper, T. Nishino, Tidal Power generation – a review of hydrodynamic modelling, in: Proceedings of the Institute of Mechanical Engineers Part a: Journal of Power and Energy, 2015, <http://dx.doi.org/10.1177/0957650915570349>.
- [2] T.A.A. Adcock, A.G.L. Borthwick, G.T. Houlby, The open boundary problem in tidal basin modelling with energy extraction, in: G.A. Aggidis, D.S. Benzon (Eds.), In Proceedings of the 9th European Wave and Tidal Energy Conference, Southampton, UK, 2011.
- [3] G.A. Aggidis, O. Feather, Tidal range turbines and generation on the Solway Firth, Renew. Energy 43 (2012) 9–17.
- [4] R. Ahmadian, R.A. Falconer, B. Lin, Hydro-environmental modelling of the

- proposed Severn barrage, UK, Proc. Institution Civ. Eng. - Energy 163 (3) (2010) 10–17.
- [5] K. Anastasiou, C.T. Chan, Solution of the 2D shallow water equations using the finite volume method on unstructured triangular meshes, *Int. J. Numer. Methods Fluids* 24 (1997) 1225–1245.
- [6] A. Angeloudis, R. Ahmadian, R.A. Falconer, B. Bockelmann-Evans, Numerical model simulations for optimisation of tidal lagoon schemes, *Appl. Energy* 165 (2016) (2016a) 522–536.
- [7] A. Angeloudis, R.A. Falconer, S. Bray, R. Ahmadian, Representation and operation of tidal energy impoundments in a coastal hydrodynamic model, *Renew. Energy* 99 (2016b) 1103–1115.
- [8] Y.H. Bae, O.K. Kyeong, H.C. Byung, Lake Sihwa tidal power plant project, *Ocean. Eng.* 37 (5–6) (2010) 454–463.
- [9] A.C. Baker, Tidal power, *Proc. Institution Electr. Eng.* 134 (A5) (1987) 392–398.
- [10] A.C. Baker, J. Walbancke, P. Leache, Tidal lagoon power generation scheme in Swansea Bay, A Rep. behalf Dep. Trade Industry Welsh Dev. Agency (2006).
- [11] S. Bray, R. Ahmadian, R.A. Falconer, Impact of representation of hydraulic structures in modelling a Severn barrage, *Comput. Geosciences* 89 (2016) (2016) 96–106.
- [12] R. Burrows, I.A. Walkington, N.C. Yates, T.S. Hedges, J. Wolf, J. Holt, The tidal range energy potential of the West Coast of the United Kingdom, *Appl. Ocean Res.* 31 (4) (2009a) 229–238.
- [13] R. Burrows, I.A. Walkington, N.C. Yates, T.S. Hedges, M. Li, J.G. Zhou, J. Wolf, J. Holt, R. Proctor, Tidal energy potential in UK waters. Proceedings of the institution of civil engineers, *Marit. Eng.* 162 (MA4) (2009b) 155–164.
- [14] A. Cornett, J. Cousineau, I. Nistor, Assessment of hydrodynamic impacts from tidal power lagoons in the Bay of Fundy, *Int. J. Mar. Energy* 1 (2013) (2013) 33–54.
- [15] Department of Energy and Climate Change (DECC), Severn tidal Power Feasibility Study: conclusions and Summary Report. Ref:10D/808, 2010.
- [16] R.A. Falconer, Y. Chen, An improved representation of flooding and drying and wind stress effects in a 2D tidal numerical model, in: Proceedings of the Institution of Civil Engineers Part 2, 1991, pp. 659–672.
- [17] C. Garrett, D. Greenberg, Predicting changes in tidal regime: the open boundary problem, *J. Phys. Oceanogr.* 7 (1977) 171–181.
- [18] S.K. Godunov, A Difference Method for the Numerical Calculation of Discontinuous Solutions of Hydrodynamic Equations. *Matemstichesky Sbornik* 47, US Joint Publications Research Service, 1959.
- [19] P. Jeffcoate, P. Stansby, D. Apsley, Flow due to multiple jets downstream of a barrage: experiments, 3D Computational Fluid Dynamics and depth-averages modelling, *J. Hydraulic Eng.* 139 (7) (2013) 754–762.
- [20] M. Kadiri, R. Ahmadian, B. Bockelmann-Evas, W. Rauen, R.A. Falconer, A review of the potential water quality impacts of tidal renewable energy systems, *Renew. Sustain. Energy Rev.* 16 (1) (2012) 329–341.
- [21] R. Kirby, The evolution of the fine sediment regime of the Severn Estuary and Bristol Channel, *Biol. J. Limnol. Soc.* 51 (1994) 37–44.
- [22] R. Kirby, W.R. Parker, Distribution and behaviour of the fine sediment in the severn estuary and inner Bristol Channel, UK. *Can. J. Fish. Aquatic Sci.* 40 (1) (1983) 83–95.
- [23] C. Peters, Severn Estuary Tidal Power. National Assembly for Wales Paper Number 10/010, 2010.
- [24] S. Petley, G. Aggidis, Swans. Bay tidal lagoon Annu. energy estimation' *Ocean. Eng.* 111 (2016) (2016) 348–357.
- [25] D. Prandle, Simple theory for designing tidal power schemes, *Adv. Water Resour.* 7 (1) (1984) 21–27.
- [26] D. Prandle, Design of tidal barrage power schemes. Proceedings of the institution of civil engineers, *Marit. Eng.* 162 (MA4) (2009) 147–153.
- [27] A. Roberts, B. Thomas, P. Sewell, Z. Khan, S. Balmain, J. Gillman, Current tidal power technologies and their suitability for applications in coastal and marine areas, *J. Ocean Eng. Mar. Energy* 2 (2) (2016) 227–245.
- [28] P.L. Roe, Approximate Riemann solvers, parameter vectors and difference schemes, *J. Comput. Phys.* 43 (1981) 357–372.
- [29] O. Sang-Ho, K.S. Lee, W. Jeung, Three-dimensional experiment and numerical simulation of the discharge performance of sluice passageway for tidal power plant, *Renew. Energy* 92 (2016) (2016) 462–473.
- [30] B.F. Sanders, Non-reflecting boundary flux function for finite volume shallow-water models, *Adv. Water Resour.* 25 (2002) (2002) 195–2002.
- [31] Severn Tidal Power Group, The Severn Barrage Project: General Report, 1989. Energy Paper Number 57, Department of Energy, HMSO, London.
- [32] Severn Embryonic Technologies Scheme (SETS) Summary report, Concept Des. a very-low head dual generation, tidal scheme Severn barrage 1 (2010) (2010). DNS 159636, Issue 1.
- [33] P.A. Sleigh, P.H. Gaskell, M. Berzins, N.G. Wright, An unstructured finite-volume algorithm for predicting flow in rivers and estuaries, *Comput. Fluids* 27 (4) (1998) 479–508.
- [34] Tidal Lagoon Power, Tidal Lagoon Swansea Bay Project Information, 2015. Online]. Available, http://tidallagoon.opendebate.co.uk/files/TidalLagoon/Project_introductiontoTidal_Lagoon_Swansea_Bay.pdf. accessed 26.02.16.
- [35] Tidal Lagoon Power, Welcome to Tidal Lagoon Cardiff's Website, 2014, 2015. Online]. Available, <http://www.tidallagooncardiff.com>. accessed 26.02.16.
- [36] N. Yates, I. Walkington, R. Burrows, J. Wolf, Appraising the extractable tidal energy resource of the UK's western coastal waters, *Philosophical Trans. R. Soc. A* 371 (2013a) 20120181.
- [37] N. Yates, I. Walkington, R. Burrows, J. Wolf, The energy gains realisable through pumping for tidal range energy schemes, *Renew. Energy* 58 (2013) (2013b) 79–84.
- [38] R.J. Uncles, Physical properties and processes in the Bristol Channel and severn estuary, *Mar. Pollut. Bull.* 61 (2010) 5–20.
- [39] B. van Leer, Towards the ultimate conservative difference scheme, *J. Comput. Phys.* 135 (2) (1997) 229–248.
- [40] S. Waters, G. Aggidis, Over 2000 years in review: revival of the archimedes screw from pump to turbine, *Renew. Sustain. Energy Rev.* 51 (2015) 497–505.
- [41] S. Waters, G. Aggidis, Tidal range technologies and state of the art in review, *Renew. Sustain. Energy Rev.* 59 (2016) (2016a) 514–529.
- [42] S. Waters, G. Aggidis, A world first: Swansea Bay tidal lagoon in review, *Renew. Sustain. Energy Rev.* 56 (2016) (2016b) 916–921.
- [43] J. Wolf, I.A. Walkington, J. Holt, R. Burrows, Environmental impacts of tidal power schemes. Proceedings of the Institution of Civil Engineers, *Marit. Eng.* 162 (MA4) (2009) 165–177.
- [44] J. Xia, R.A. Falconer, B. Lin, Impact of different tidal renewable energy projects on the hydrodynamic processes in the Severn Estuary, UK, *Ocean. Model.* 32 (1–2) (2010a) 86–104.
- [45] J. Xia, R.A. Falconer, B. Lin, Impact of different operating modes for a Severn Barrage on the tidal power and flood inundation in the Severn Estuary, *Appl. Energy* 87 (7) (2010b) 2374–2391.
- [46] J. Xia, R.A. Falconer, B. Lin, Hydrodynamic impact of a tidal barrage in the Severn Estuary, UK, *Renew. Energy* 35 (7) (2010c) 1455–1468.
- [47] J. Zhou, R.A. Falconer, B. Lin, Refinements to the EFDC model for predicting the hydro-environmental impacts of a barrage across the Severn Estuary, *Renew. Energy* 62 (2014) (2014a) 490–505.
- [48] J. Zhou, S. Pan, R.A. Falconer, Effects of open boundary location on the far-field hydrodynamics of a Severn Barrage, *Ocean. Model.* 73 (2014) (2014b) 19–29.
- [49] J. Zhou, S. Pan, R.A. Falconer, Optimisation modelling of the impacts of a Severn Barrage for a two-way generation scheme using a Continental Shelf model, *Renew. Energy* 72 (2014) (2014c) 415–427.
- [50] G.A. Aggidis, D.S. Benzon, Operational optimisation of a tidal barrage across the Mersey Estuary using 0-D modelling, *Ocean Eng.* 66 (2013) 69–81.
- [51] R.A. Falconer, J. Xia, B. Lin, R. Ahmadian, The Severn Barrage and other tidal energy options: hydrodynamic and power output modelling, *Sci. China Ser. E Technol. Sci.* 52 (11) (2009) 3414–3424.